

tion; $\theta = (T_w - T)/(T_w - T_0)$, $\omega = u/u_0$, relative temperature and velocity, respectively; δ , δ_T , thickness of the dynamic and thermal boundary layers, respectively; $\epsilon_1 = (\delta/\delta_T)^{n_T n}$, coefficient of nonsimilarity of velocity and temperature profiles; n and n_T , indices for power law approximation to the velocity and temperature profiles, respectively; T_w and T_0 , temperatures of the wall and of the main air flow.

LITERATURE CITED

1. A. I. Leont'ev, V. G. Puzach, V. P. Komarov, I. K. Ermolaev, N. V. Dubina, and V. A. Fadeev, *Inzh.-Fiz. Zh.*, **33**, No. 2 (1977).
2. S. S. Kutateladze and A. I. Leont'ev, *Turbulent Boundary Layers in Compressible Gases*, Academic Press (1964).

NUMERICAL ANALYSIS OF LAMINAR FLUID FLOW IN A "POROUS PIPE IN A PIPE" HEAT EXCHANGER

V. A. Babenko and D. K. Khrustalev

UDC 532.517.2:536.27

The change in the velocity of liquid overflow through the wall of a porous tube along the length of a system as a function of the input flow parameters and the permeability of the inner tube walls is investigated.

A flow with variable rate along pipes of different configurations was recently the theme of a considerable number of publications, which has certainly been caused by the demands of engineers analyzing such flows. Motion with mass varying along the path is realized in collector systems, e.g., in heat exchangers with porous elements, in heat pipes, etc. Laminar fluid flow in a porous pipe with constant suction along the length has been studied in [1-5]. A flow with rate of mass delivery or extraction varying according to a known law has been studied considerably less [6-8]. A more complex case is examined in this paper — flow with variable mass in two channels separated by a permeable baffle. The velocity of overflow from one channel to the other is not known and is determined from the solution of the problem. The viscosity and density of the fluid are hence considered constant, mechanical energy dissipation into heat is neglected, and the geometric dimensions of the system are such that the channel length is substantially greater than its diameter.

Laminar incompressible fluid flow in a circular pipe with permeable walls of a porous material inserted in a coaxial pipe of larger radius with impermeable walls is considered.

Under the effect of a pressure drop on the porous pipe wall, the fluid will be sucked out of the inner channel into the outer or conversely. The pressure drop on the wall and the overflow velocity depend on the axial coordinate. Let us take Darcy's law for porous material as the dependence of the overflow on the pressure drop. The suction rate for a homogeneously porous wall with constant thickness can be expressed as follows according to Darcy's law:

$$v_{|r=a} = \frac{K(p_{|r=a} - p_{|r=b})}{\mu a \ln \frac{b}{a}} \quad (1)$$

The flows in the inner channel and in the annular gap are described by the stationary Navier-Stokes equations:

$$\begin{aligned} u^{(i)} \frac{\partial u^{(i)}}{\partial x} + v^{(i)} \frac{\partial u^{(i)}}{\partial r} &= -\frac{1}{\rho} \frac{\partial p^{(i)}}{\partial x} + \nu \left(\frac{\partial^2 u^{(i)}}{\partial x^2} + \frac{1}{r} \frac{\partial u^{(i)}}{\partial r} + \frac{\partial^2 u^{(i)}}{\partial r^2} \right), \\ u^{(i)} \frac{\partial v^{(i)}}{\partial x} + v^{(i)} \frac{\partial v^{(i)}}{\partial r} &= -\frac{1}{\rho} \frac{\partial p^{(i)}}{\partial r} + \nu \left(\frac{\partial^2 v^{(i)}}{\partial x^2} + \frac{1}{r} \frac{\partial v^{(i)}}{\partial r} + \frac{\partial^2 v^{(i)}}{\partial r^2} \right), \end{aligned} \quad (2)$$

A. V. Lykov Institute of Heat and Mass Transfer, Academy of Sciences of the Belorussian SSR, Minsk. Translated from *Inzhenerno-Fizicheskii Zhurnal*, Vol. 36, No. 5, pp. 779-786, May, 1979. Original article submitted April 4, 1978.

$$r \frac{\partial u^{(i)}}{\partial x} + \frac{\partial}{\partial r} (rv^{(i)}) = 0, \quad i = 1, 2, \quad (3)$$

where the superscript $i = 1$ refers to the inner, and 2 to the outer channel, and (3) is the continuity equation.

It is assumed that the mean radial velocity is small compared to the mean axial velocities in both channels, i.e., $\bar{v}/\bar{u} \ll 1$. Applying an analysis on the order of smallness to the Navier-Stokes equations, we obtain equations agreeing in form with the boundary-layer equations in a first approximation, as is usual.

Let us introduce the following notations:

$$z = \frac{vx}{a^2 u_{01}}, \quad R = \frac{r}{a}, \quad U = \frac{u}{u_{01}}, \quad (4)$$

$$P = \frac{p}{\rho u_{01}^2}, \quad A = \frac{K \bar{u}_{01}}{v^2 \ln \frac{b}{a}}, \quad V = \frac{va}{v}.$$

We then obtain a system of Prandtl equations in cylindrical coordinates for the dimensionless quantities:

$$U^{(i)} \frac{\partial U^{(i)}}{\partial z} + V^{(i)} \frac{\partial U^{(i)}}{\partial R} = - \frac{dP^{(i)}}{dz} + \frac{\partial^2 U^{(i)}}{\partial R^2} + \frac{1}{R} \frac{\partial U^{(i)}}{\partial R}, \quad (5)$$

$$R \frac{\partial U^{(i)}}{\partial z} + \frac{\partial}{\partial R} (RV^{(i)}) = 0, \quad i = 1, 2. \quad (6)$$

Let us add the mass conservation laws in integral form for each domain to the boundary-layer equations:

for the inner channel

$$\frac{d}{dz} \int_0^1 U^{(1)} R dR = -V_{|R=1}^{(1)}, \quad (7)$$

for the annular gap

$$\frac{d}{dz} \int_{\frac{b}{a}}^{\frac{c}{a}} U^{(2)} R dR = V_{|R=\frac{b}{a}}^{(2)}, \quad (8)$$

for the porous wall

$$\frac{b}{a} V_{|R=\frac{b}{a}}^{(2)} = V_{|R=1}^{(1)}. \quad (9)$$

Let us write the boundary conditions reflecting the symmetry of the problem and the adhesion of the fluid to the walls

$$V_{|R=0}^{(1)} = 0, \quad \left. \frac{\partial U^{(1)}}{\partial R} \right|_{R=0} = 0, \quad U_{|R=1}^{(1)} = 0, \quad U_{|R=\frac{b}{a}}^{(2)} = U_{|R=\frac{c}{a}}^{(2)} = 0, \quad (10)$$

$$V_{|R=\frac{c}{a}}^{(2)} = 0, \quad U_{|z=0}^{(i)} = \frac{f_i(R)}{u_{01}}, \quad V_{|z=0}^{(i)} = \frac{\varphi_i(R) a}{v}, \quad i = 1, 2,$$

where $f_i(R)$, $\varphi_i(R)$ are functions giving the velocity profiles $u^{(i)}$ and $v^{(i)}$ at the entrance.

Let us define the Reynolds numbers used later for the overflow and the longitudinal velocities in both domains:

$$Re_r = \frac{v_{|r=a} a}{v} = V_{|R=1}^{(1)}, \quad Re_1 = \frac{\bar{u}^{(1)} a}{v}, \quad Re_2 = \frac{\bar{u}^{(2)} \sqrt{c^2 - b^2}}{v}. \quad (11)$$

The problem was numerically solved by using the finite-difference method. An implicit finite-difference approximation of the equations which assured the stability for any relation-

ship between the z and R spacings for $U \geq 0$ [2] was used for the solution. The equations were approximated on a uniform mesh in each domain. The spacings along the radius in the inner and outer channels were selected different. The velocities and pressures were considered known for any k and l in the layer j and above in the flow. The flow is unknown on the $(j + 1)$ -th layer. There were no iterations in the nonlinearity.

Let us use the following finite-difference representations of the terms in (5) and (6) for the $(j + 1)$ -th layer:

$$\begin{aligned} \frac{\partial U}{\partial z} &= \frac{U_{j+1,k} - U_{j,k}}{\Delta z}, & \frac{\partial U}{\partial R} &= \frac{U_{j+1,k+1} - U_{j+1,k-1}}{2\Delta R}, \\ \frac{\partial^2 U}{\partial R^2} &= \frac{U_{j+1,k+1} - 2U_{j+1,k} + U_{j+1,k-1}}{(\Delta R)^2}, & \frac{\partial P}{\partial z} &= \frac{P_{j+1} - P_j}{\Delta z}. \end{aligned} \quad (12)$$

Consequently, we obtain a system of algebraic equations from (5):

$$\alpha_{j,k} U_{j+1,k-1}^{(1)} + \beta_{j,k} U_{j+1,k}^{(1)} + \gamma_{j,k} U_{j+1,k+1}^{(1)} = \Phi_{j,k} - \frac{\partial P^{(1)}}{\partial z}, \quad (13)$$

$$\alpha_{j,l} U_{j+1,l-1}^{(2)} + \beta_{j,l} U_{j+1,l}^{(2)} + \gamma_{j,l} U_{j+1,l+1}^{(2)} = \Phi_{j,l} - \frac{\partial P^{(2)}}{\partial z}, \quad (14)$$

where

$$\begin{aligned} \alpha_{j,i} &= \frac{1}{2R_i \Delta R} - \frac{V_{j,i}}{2\Delta R} - \frac{1}{(\Delta R)^2}; \\ \beta_{j,i} &= \frac{2}{(\Delta R)^2} + \frac{U_{j,i}}{\Delta z}, \\ \gamma_{j,i} &= \frac{V_{j,i}^2}{2\Delta R} - \frac{1}{(\Delta R)^2} - \frac{1}{2R_i \Delta R}, \quad \Phi_{j,i} = \frac{U_{j,i}^2}{\Delta z}, \end{aligned}$$

for the domain 1, $i = k = 1, 2, 3, \dots, n$ and for the domain 2, $i = l = 0, 1, 2, 3, \dots, m$.

Resolving the indeterminacy by L'Hospital's rule for $R = 0$, we obtain

$$\alpha_{j,0} = \frac{U_{j,0}^{(1)}}{\Delta z} + \frac{4}{(\Delta R)^2}, \quad \beta_{j,0} = -\frac{4}{(\Delta R)^2}, \quad \Phi_{j,0} = \frac{U_{j,0}^{(1)2}}{\Delta z}, \quad \gamma_{j,0} = 0.$$

Let us write the continuity equation (6) in finite-difference form:

$$\frac{R_k (U_{j+1,k}^{(i)} - U_{j,k}^{(i)}) + R_{k+1} (U_{j+1,k+1}^{(i)} - U_{j,k+1}^{(i)})}{2\Delta z} + \frac{V_{j+1,k+1}^{(i)} R_{k+1} - V_{j+1,k}^{(i)} R_k}{\Delta R} = 0, \quad (15)$$

for $i = l, k = 1, 2, \dots, n$ while $k = 0, 1, 2, \dots, m$ for $i = 2$. Applying L'Hospital's rule for $R = 0$, we have

$$\frac{U_{j+1,1}^{(i)} + U_{j+1,0}^{(i)} - U_{j,1}^{(i)} - U_{j,0}^{(i)}}{2\Delta z} + \frac{2V_{j+1,1}^{(i)}}{\Delta R} = 0. \quad (16)$$

Summing (15) and (16) for the inner channel and taking into account that

$$V_{j+1,n+1} \equiv V_{j,R=1} = A(P_{j+1}^{(1)} - P_{j+1}^{(2)}),$$

we obtain

$$\frac{\Delta z}{\Delta R} A(P_{j+1}^{(1)} - P_{j+1}^{(2)}) + \sum_{k=2}^n R_k U_{j+1,k}^{(1)} + \frac{3}{4n} U_{j+1,1}^{(1)} + \frac{1}{4n} U_{j+1,0}^{(1)} = \sum_{k=2}^n R_k U_{j,k}^{(1)} + \frac{3}{4n} U_{j,1}^{(1)} + \frac{1}{4n} U_{j,0}^{(1)}. \quad (17)$$

Relationship (17) expresses the law of conservation of mass in integral form for the first domain and therefore corresponds to (7). Relationship (16) is not used later; (15) and (17) can be considered linearly independent.

Analogously, from (15) we have an expression reflecting the mass conservation in the annular gap

$$-\frac{\Delta z}{\Delta R} A (P_{j+1}^{(1)} - P_{j+1}^{(2)}) + \sum_{l=1}^m R_l U_{j+1,l}^{(2)} = \sum_{l=1}^m R_l U_{j,l}^{(2)}. \quad (18)$$

We have therefore obtained a system of algebraic equations (13)-(15), (17), (18) in which the number of unknowns $U_k^{(1)}$, $U_l^{(2)}$, $V_k^{(1)}$, $V_l^{(2)}$, $P^{(1)}$, $P^{(2)}$ agrees with the number of equations.

Let us seek the velocities $U_k^{(1)}$, $U_l^{(2)}$ in the form of a sum of two components:

$$U_{j+1,k}^{(1)} = N_{j+1,k}^{(1)} + W_{j+1,k}^{(1)} \frac{\partial P^{(1)}}{\partial z}, \quad U_{j+1,l}^{(2)} = N_{j+1,l}^{(2)} + W_{j+1,l}^{(2)} \frac{\partial P^{(2)}}{\partial z} \quad (19)$$

Substituting these expressions into (13), (14) for $N^{(1)}$, $N^{(2)}$, $W^{(1)}$, $W^{(2)}$, we obtain four systems of algebraic equations

$$\alpha_{j,k} N_{j+1,k-1}^{(i)} + \beta_{j,k} N_{j+1,k}^{(i)} + \gamma_{j,k} N_{j+1,k+1}^{(i)} = \frac{U_{j,k}^{(i)2}}{\Delta z},$$

$$\alpha_{j,k} W_{j+1,k-1}^{(i)} + \beta_{j,k} W_{j+1,k}^{(i)} + \gamma_{j,k} W_{j+1,k+1}^{(i)} = -1, \quad i=1, 2, \quad (20)$$

where the coefficients α , β , γ are the same as in (13) and (14).

Directly at the walls $\alpha = \gamma = 0$, $\beta = 1$ for each of systems (20).

It is convenient to solve system (20) by factorization. By evaluating $N^{(i)}$, $W^{(i)}$ and substituting (19) into (17) and (18), we obtain two equations with two unknowns $P_{j+1}^{(1)}$ and $P_{j+1}^{(2)}$. Having determined the pressure on the (j+1)-th layer in both domains, we find the longitudinal components of the velocity vector $U^{(i)}$ from (19). We find the suction Reynolds number $Re_V \equiv V_{iR=1}^{(1)}$ for a known pressure drop on the porous wall. The velocities $V_k^{(1)}$, $V_l^{(2)}$ are determined from recursion relation (15).

After this we go over to the next layer j and repeating the process compute the velocity field for the whole structure in this manner.

The problem was solved for a heat exchanger with the following geometric dimensions: $a = 9 \cdot 10^{-3}$ m; $b = 20 \cdot 10^{-3}$ m; $c = 25 \cdot 10^{-3}$ m; $L = 3$ m. The main computational mesh had 100 nodes along the length of the structure and 50 along the radius in the inner and annular channels. The change in the computation results did not exceed 1% when the mesh was reduced two and more times in size.

A checking computation was performed for the case of impermeable inner tube walls and a steady velocity profile at the entrance. Hence, the velocity profiles were practically unchanged with distance from the entrance. The pressure drop in the inner channel agreed with the drop computed by the Poiseuille formula to hundredths of a percent accuracy. The results of variant No. 2 (see Table 1) were compared with values of U, V, P, which were obtained by the method proposed by Weissberg [1] for the computation of the flow in a pipe with permeable walls with constant suction. It was hence assumed that $Re_V = 0.63$ over the whole length of the structure. The differences in the values of U, V, P in the inner channel were less than 0.5%.

The proposed finite-difference scheme describes well such physical phenomena as pressure restoration and the occurrence of reverse flows under strong suction, and reconstruction of the pivotal velocity profile in the entry section.

It can therefore be considered that the results obtained by this method have sufficient accuracy.

The solution of the problem showed that the overflow distribution in the system depends essentially on the magnitude of the inner pipe wall permeability and on the velocity profiles at the entrance.

Homogeneous (pivotal) and Poiseuille (steady) profiles were examined. The velocity field at the entrance is homogeneous if the structure is attached directly to the pressure source, a pump or plenum.

A steady velocity profile holds when a sufficiently long section with impermeable walls adjoins the structure entrance. It is given by the formulas

TABLE 1. Initial Data for Different Variants of the Computation for $\nu = 0.2323 \cdot 10^{-6} \text{ m}^2/\text{sec}$; $\rho = 136 \text{ kg/m}^3$

Variant number	K , Darcy	$Re_1 (x=0)$	$Re_2 (x=0)$	$(p^{(1)} - p^{(2)}) (x=0)$, N/m^2
1	0	1500	900	3,75
2	1	1500	900	3,75
3	5	800	1700	0,75
4	10	1300	1600	0,375
5	20	1000	1670	0,25
6	30	1200	1850	0,125

$$f_1(R) = 2\bar{u}_{01}(1 - R^2), \quad f_2(R) = \bar{u}_{02} \frac{\frac{R^2 a^2 - b^2}{4} + \frac{b^2 - c^2}{4 \ln(c/b)} \ln\left(\frac{Ra}{b}\right)}{\frac{c^2 - b^2}{4 \ln(c/b)} - \frac{b^2 + c^2}{3}}, \quad (21)$$

for the homogeneous profile $f_i(R) = \text{const}(i)$, $i = 1, 2$.

Let us note that if the value $V_{iR=1}^{(1)}$ is known for the layer j , then by limiting ourselves to the case of zero longitudinal component of the velocity vector in the porous wall, we can find the magnitude of the velocity V in the porous domain as a function of the radius by means of the formula

$$V(R) = V_{iR=1}^{(1)}/R. \quad (22)$$

The set of initial data for the different computational variants is presented in Table 1.

The dashed lines in the figures correspond to the pivotal profile at the entrance.

Steady Entrance Velocity Profile

Suction of the fluid from the inner channel causes a certain pressure rise while blowing in the outer channel specifies a pressure drop (Fig. 1). The influence of suction on the pressure distribution reduces to the fact that it is impossible to obtain strictly constant suction along the length for this structure. However, cases of almost constant suction are possible for small K (Fig. 2).

Growth of suction along the length is necessary to stabilize the temperature field in the porous domain since the fluid moving away from the entrance will be heated somewhat because of internal heat liberation and the influx of heat from outside. Cases of growing suction are shown in Fig. 2.

Pivotal Entrance Velocity Profile

Reconstruction of the velocity field occurs upon giving a homogeneous velocity profile at the entrance, which results in substantial differences in the overflow velocity as compared with the case considered above. Upon withdrawal from the entrance, the velocity profile

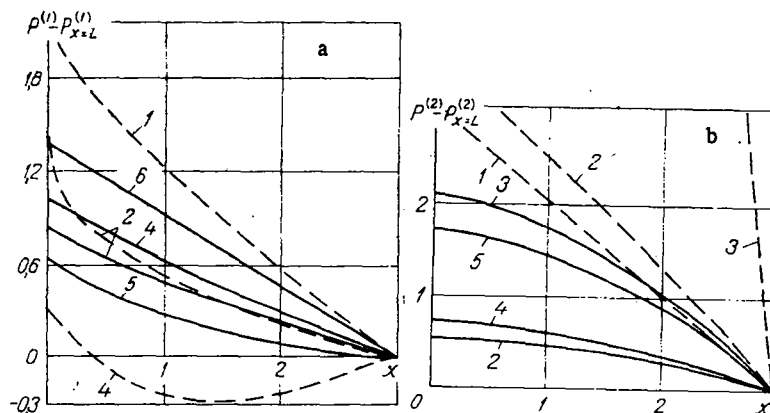


Fig. 1. Pressure change in the inner (a) and outer (b) channels along the structure length. Numbers at the curves signify the variant.

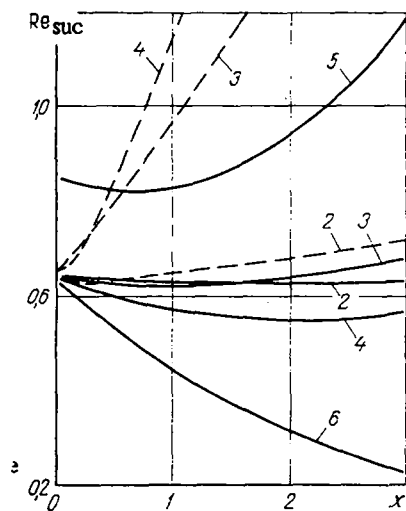


Fig. 2

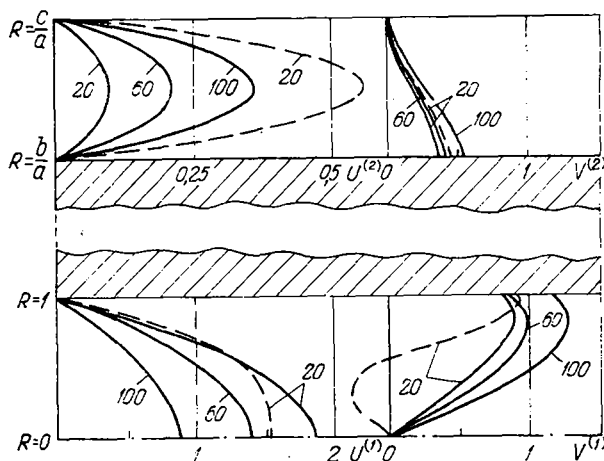


Fig. 3

Fig. 2. Change in magnitude of the suction along the structure length.

Fig. 3. Velocity profiles $U^{(1)}$, $U^{(2)}$, $V^{(1)}$, $V^{(2)}$ at different distances from the entrance. Numbers at the curves signify the number of the layers along the system axis.

in both domains gradually approaches the steady state, whereupon negative radial velocities occur (Fig. 3).

Reconstruction of the velocity field results in the pressure at the entrance changing more sharply than at some distance away. The pressure gradient in the annular gap is greater than in the inner channel (Fig. 1b).

The total friction drag for this structure is considerably greater in the case of a pivotal profile at the entrance than for the steady state.

The presence of a fluid overflow results in a rise in the total friction drag; for $Re_v = 0.63$ it grew 8% as compared with the case of zero suction.

Reconstruction of the velocity field complicates the prediction of the mode of mass overflow from one channel to the other under different conditions at the entrance. Nevertheless, even in the case of a pivotal profile at the entrance the production of stable modes in this structure is possible (Fig. 2).

In conclusion, let us note that the proposed computation method can be used for any entrance velocity profiles for $U \geq 0$.

NOTATION

k, l , radial indices in the inner and outer channels; j , index along the system length; n and m , quantity of partitions along the radius in the inner and outer channels; u and v , longitudinal and radial velocity, m/sec; U and V , dimensionless longitudinal and radial velocities; p , pressure, N/m²; P , dimensionless pressure; K , permeability coefficient, Darcy; μ, ν , coefficients of dynamic (kg/m·sec) and kinematic (m²/sec) viscosity; ρ , fluid density, kg/m³; a , inner radius of the porous pipe, m; b , outer radius of the porous pipe, m; c , inner radius of the outer pipe, m; L , structure length, m; \bar{u}_{01} and \bar{u}_{02} , mean velocities at the entrance to the inner and outer channels, m/sec; r , radius, m; x , distance from the entrance, m; R , dimensionless radius; z , dimensionless distance from the entrance; Re_1 and Re_2 , Reynolds number for the inner and outer channels; Re_r , suction Reynolds number.

LITERATURE CITED

1. H. L. Weissberg, *Phys. Fluids*, **2**, 510 (1959).
2. A. S. Berman, *Proceedings of Second International Conference on the Peaceful Uses of Atomic Energy*, Paper NP-720, Geneva, **4**, 351 (1958).
3. C. A. Busse, *Thermionic Conversion Special Conference*, Palo Alto, California (1967).
4. S. W. Yuan and A. B. Finkelstein, *Trans. ASME*, **78**, 719-724 (1956).

5. R. W. Hornbeck, W. T. Rouleau, and F. S. Osterle, *Phys. Fluids*, 6, No. 11 (1963).
6. L. S. Galowin and V. A. Barker, ASME Paper No. HT-22 (1969).
7. L. S. Galowin, L. S. Fletcher, and M. J. Desantis, *J. Heat Transfer*, No. 2, 263 (1974).
8. L. S. Galowin, L. S. Fletcher, and M. J. Desantis, AIAA Paper No. 73-725 (1973).

COMPUTATION OF THE PRESSURE LOSS IN GAS FLOW THROUGH POROUS MATERIALS

V. D. Daragan, A. Yu. Kotov,
G. N. Mel'nikov, A. V. Pustogarov,
and V. I. Starshinov

UDC 532.546:537.527

The development of methods of designing the heat shield of high-heat-stressed elements of power plants, particularly plasmatrons, by blowing coolant through permeable structure elements requires a study, firstly, of the gas flow hydrodynamics in a porous material. The rise in the specific power of a plasmatron, and hence, the thermal loading of its elements, the use of blowing through a porous wall as a method of delivering the working body into the channel [1], result in the need to use blowing with high specific gas mass flow rates. The features of flows with high specific mass flow rates are the predominance of inertial pressure losses over the viscous losses, the rise in the pressure losses at the entrance and exit from the porous wall, the necessity to take account of compressibility in describing the flow in a porous medium. A rise in the mass flow rate through a wall can result in "choking" of the flow, i.e., in a mode when the mass flow rate will remain constant for a constant pressure in front of the wall, independently of the pressure change at the exit.

The flow in porous media with compressibility taken into account is inadequately investigated. The influence of compressibility on the flow as a function of the porous material characteristics and of the magnitude of the mass flow rate is analyzed in [2, 3] on a capillary model of a porous body. The presence of "choking" effects was experimentally confirmed in [4, 5]. The influence of material porosity on the "choking" was considered in [6]. However, actual porous materials are characterized by a complex pore space, a difference in pore and interpore passage sizes, convolutions of the pore channels, which constrain the application of an analysis based on a capillary model [2, 3].

The hydraulic drag of a porous wall can be determined from the expression [7]

$$\frac{P_2 - P_1}{L} = \xi \frac{2\rho v^2}{d}, \quad (1)$$

where ξ is the hydraulic drag coefficient; P_2 and P_1 , gas pressure at the entrance and exit from a porous wall of thickness L ; and v and d , characteristic velocity and geometric size. Selection of the characteristic parameters for a porous material is ambiguous. The filtration velocity $v_f = G/\rho F$ (G is the mass flow rate through a porous wall with cross-sectional area F at a normal velocity) or the mean velocity in the pores $v_p = v_f/\Pi$, where Π is the porosity, is taken as the characteristic velocity. The particle diameter d_{par} or the mean pore diameter d_p [7] is taken as the characteristic dimension. Since ξ is a function of not only the material structure but also the flow mode $\epsilon = f(Re)$, the results for different porous materials [7] is not extended successfully by means of (1). Flow deviation from the Darcy law occurs for values of Re substantially less than should have been expected on the basis of computations for models with channels with the characteristic dimensions d_{par} and d_p taken since the passage to the inertial flow mode is determined not only by the size of the pore channels but also by the shape, convolution, contractions, and expansions. Moreover, substantial errors are inherent to the very methods for determining the mean pore and particle size.

The two-term mode of writing the fluid motion equation

$$-\frac{dP}{dx} = \alpha w + \beta \rho v^2 \quad (2)$$